ADSORPTION OF REMAZOL BRILLIANT VIOLET ONTO CHITOSAN 10B IN AQUEOUS SOLUTION: KINETICS, EQUILIBRIUM AND THERMODYNAMICS STUDIES

SUBARNA KARMAKER, AMLAN JYOTI NAG and TAPAN KUMAR SAHA[*]

Department of Chemistry, Jahangirnagar University, Savar, Dhaka-1342, Bangladesh
✉ *Corresponding author: T. K. Saha, tksaha_ju@yahoo.com*

The adsorption characteristics of Remazol Brilliant Violet (RBV) dye onto chitosan 10B were investigated in aqueous solutions as a function of solution pH, dye concentration, ionic strength and temperature, respectively. The adsorption kinetics data obtained from various batch experiments were analyzed by using pseudo-first- and pseudo-second-order, as well as Elovich and intraparticle diffusion kinetic models. The results exhibited that the sorption process obeys pseudo-second order kinetics, whereas intraparticle diffusion is the rate determining step. The equilibrium adsorption isotherm data are fitted better by the Langmuir model rather than by the Freundlich, Temkin and Dubinin-Radushkevich models. Moreover, the mean adsorption energy (E) from the Dubinin-Radushkevich isotherm and the activation energy (E_a) from the Arrhenius equation indicate that the RBV adsorption onto chitosan 10B is a physisorption process. Thermodynamic parameters, such as the changes in free energy (ΔG), enthalpy (ΔH) and entropy (ΔS), suggest that the RBV dye adsorption onto chitosan 10B in aqueous solution is spontaneous and endothermic in nature. Desorption tests were carried out in a NaOH solution (pH 12.5) and the chitosan flakes were found to be reusable.

Keywords: adsorption, kinetics, equilibrium, thermodynamics, chitosan, azo dyes

INTRODUCTION

A large number of anionic azo dyes are widely used in textile dyeing, paper printing and manufacture of pharmaceutical drugs and toys. This group of dyes dominates the world-wide market of dyestuffs with a share of about 70%.[1] They are less susceptible to oxidative catabolism and generally non-biodegradable. Only a few can be degraded microbiologically under anaerobic conditions, but in most cases, with the production of carcinogenic amines and mutagens.[2]

Conventional processes, such as adsorption, oxidation–ozonation, coagulation, coagulation–flocculation, and biological methods are adopted for removing azo dyes. Adsorption methods in solution systems play a vital role in many areas of practical environmental technology, which are mainly used in waste water treatment, due to several advantages, such as high efficiency, simple operation and easy recovery/reuse of the adsorbent.[3] Many types of adsorbent materials, such as clay minerals,[4-6] perlite,[7] biomaterials,[8,9] activated carbons[10,11] and industrial solid wastes,[12]

have been tested for the removal of azo dyes from aqueous solution. Activated carbon is extensively used as an adsorbent due to its high degree of effectiveness. However, its use is limited because of its high cost.

This has led many researchers to search for low cost and locally available adsorbents, so that the process becomes economically feasible. In recent years, biomass has been accepted as an appropriate low-cost adsorbent for the removal of dyes from aqueous solution. Many types of natural and modified biomass, such as biochars,[13] mango leaves,[14] *Daucus carota*,[15] *Irvingia gabonenses*,[16] agricultural by-products,[17] chitin,[18] chitosan[19-23] and functionalized chitosan,[24-26] have shown promising results in dye adsorption applications. However, related reports on utilizing chitosan to remove Remazol Brilliant Violet (RBV; Fig. 1a) azo dye from aqueous solution are relatively scarce. In this study, chitosan 10B (Fig. 1b) has been selected as an adsorbent to remove RBV from aqueous solution.

Chitosan is simply obtained from chitin by deacetylating its acetoamide groups with a strong alkaline solution. Chitin is generally found in wastes from the seafood processing industry, mainly shells of crabs, shrimp, prawns and krill. Shrimp shell waste is generated in huge amounts by the seafood processing industries from Bangladesh (more than 30,000 tons per year).[27] This waste is low-cost, available in abundance and suitable for producing chitin polymer. Consequently, the high proportions of amino and hydroxyl functions in chitosan make it very useful for the adsorption and removal of several dyes from industrial wastewater.

The objective of the present study has been to assess the ability of chitosan 10B to adsorb the RBV azo dye from aqueous solution and to optimize the conditions for its adsorption. Batch adsorption studies were carried out in aqueous solution as a function of solution pH, initial dye concentration, ionic strength and temperature. Various models were used to examine the adsorption kinetics, mechanism and equilibrium adsorption behavior of RBV onto chitosan 10B in aqueous solution. The reuse of chitosan 10B was investigated. The thermodynamics of the adsorption process was also studied.

EXPERIMENTAL
Chemicals and preliminary characterization of chitosan
Chitosan 10B (100% deacetylated chitin, Katokichi Bio Co. Ltd., Japan) was used without further purification. The mass median diameters of the chitosan 10B flakes were estimated to be of 228 ±5 µm, using a laser scattering particle size analyzer (LDSA-240DA, Tonichi Computer Applications, Japan), equipped with a dry dispersing apparatus (PD-IOS, Tonichi Computer Applications, Japan).

The dye Remazol Brilliant Violet (RBV) was bought from Sigma-Aldrich, Germany, and was used without further purification. The chemical structure of RBV is shown in Figure 1a. The other reagents used in this study were of pure analytical grade. Deionized water was prepared by passing distilled water through a deionizing column (Barnstead, Syboron Corporation, Boston, USA).
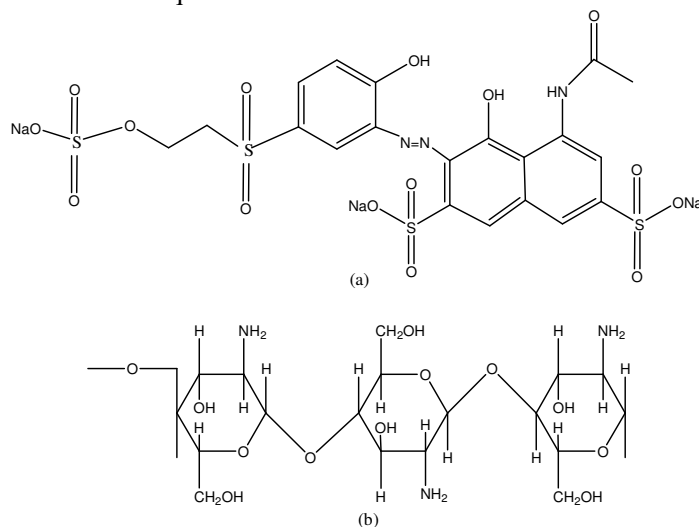

Figure 1: Structures of (a) chitosan 10B and (b) Remazol Brilliant Violet (RBV)

Batch adsorption experiments
In order to estimate the adsorption characteristics of RBV onto chitosan 10B flakes, batch adsorption studies were carried out in 125 mL stoppered bottles containing a fixed amount (0.05 g) of adsorbent and 25 mL of 100 µmol/L dye solution.[20] The initial pH of the solution was adjusted with 1 mol/L HCl or 1 mol/L NaOH solution, by using a pH meter (HANNA Instruments Microprocessor pH meter). The stoppered bottles were agitated in a thermostated shaker at room temperature (31 ± 0.2 °C), with a speed of 120 r/min, until reaching equilibrium. Each bottle was capped to avoid evaporation at high temperature. Samples were withdrawn at desired time intervals for analyzing the concentration of RBV in the solution. The samples were centrifuged at a speed of 4000 r/min for 5 min. The concentration of RBV in the supernatant was determined by the spectrophotometric method, using a Shimadzu UV-1601PC spectrophotometer (Shimadzu, Japan), at λ_{max} value of 559 nm. The λ_{max} (559 nm) of the RBV solution was found to be constant in the pH range between 4 and 12. The apparent molar absorptivity of RBV was estimated to be 8.6×10^3 L/mol/cm at 559 nm and pH 4-12. The amount of RBV adsorbed at time t, q_t (µmol/g) was determined by:

$$q_t = \frac{V(C_0 - C_t)}{m}$$
(1)

where C_0 (µmol/L) and C_t (µmol/L) are the liquid-phase concentrations of RBV at initial and at any time t, respectively, V (L) is the volume of the RBV solution and m (g) is the amount of dry chitosan 10B flakes used.

The adsorption kinetics was also investigated varying the initial concentration of the dye solutions (75-200 µmol/L), ionic strength (0.01-0.04 mol/L) and temperature (36, 41 and 46 °C), respectively. The ionic strength of the dye solutions was adjusted with 1 mol/L Na_2SO_4 solution. Equilibrium adsorption was performed at different temperatures of 31, 36, 41 and 46 °C, and at pH 4 in the absence of Na_2SO_4.

The amount of RBV dye adsorbed onto chitosan 10B at equilibrium time, q_e (µmol/g), was determined by:

$$q_e = \frac{V(C_0 - C_e)}{m}$$
(2)

where C_e (µmol/L) is the liquid-phase concentration of RBV at equilibrium time; C_0, V and m remain the same as described above.

In the desorption study, 25 mL of 0.1 mol/L NaOH solution was used to desorb RBV from the chitosan 10B flakes. The adsorbent was contacted with 25 mL of 100 µmol/L RBV solution for 120 min, filtered and then dried at room temperature (31 °C) overnight. The dye loaded-adsorbent was transferred into 25 mL desorbing solution and the mixture was stirred for 120 min. The amount of adsorption was determined in the same way as described above. All the data presented in this paper are the mean of double measurements.

RESULTS AND DISCUSSION
Adsorption kinetics
Effect of pH on adsorption kinetics

In this work, the effect of pH on the adsorption kinetics of RBV onto chitosan 10B flakes was studied in aqueous solution while the initial dye concentration, shaking time, amount of chitosan 10B and temperature were fixed at 100 µmol/L, 120 min, 0.05 g and 31 °C, respectively. The results of pH effects on the adsorption kinetics of RBV by the chitosan 10B are presented in Figure 2. The initial dye adsorption rate, h (µmol/g min), and the amount of equilibrium dye adsorption, q_e (µmol/g), decreased significantly with increasing solution pH (Table 1). We noticed that the dye uptake reached equilibrium within 10 min at pH 4-5, 30 min at pH 6-9 and 45 min at pH 10-12, respectively (Fig. 2). However, the data were taken for 120 min to ensure that complete equilibrium was established. The amount of equilibrium dye adsorption (q_e) was found to be 58.25 µmol/g at pH 4 and 31.78 µmol/g at pH 12,

respectively. These results can be explained on the basis of the charge developed over the surface of the adsorbent and dye ions as a result of the variation in the solution pH. It has been reported that the pH_{zpc} of chitosan is 6.3, and it undergoes 99% protonation at pH 4.3.[20] It is expected that positively charged functional groups on the adsorbent surface will favor the adsorption of negatively charged dye anions due to electrostatic attraction. At acidic pH values, the electrostatic attractions enhanced between the dye anions and the adsorption sites of chitosan, and dye adsorption increased. However, the positively charged sites of chitosan diminish with the increment of pH, and the surface of chitosan becomes negatively charged. This situation does not benefit the adsorption of anionic dye and causes electrostatic repulsion. Hydroxyl ions are in competition with dye ions at high pH, and the adsorption of the dye from aqueous solution decreases. Similar results were observed in the adsorption of anionic dyes in aqueous solution onto several other adsorbents.[17,20,22] Hence, the pH of the aqueous solution plays a significant role on the adsorption rate and the amount of equilibrium RBV dye adsorption onto chitosan 10B (Table 1). The appropriate pH was found to be 4, in the observed pH range from 4 to 12, and hence, pH 4 was selected for performing subsequent experiments.

Effect of initial dye concentration on adsorption kinetics

The effects of initial dye concentration on the adsorption kinetics of RBV onto chitosan 10B in aqueous solution (pH 4) at room temperature (31 °C) are shown in Figure 3. It is observed that the dye adsorption was fast for the first 7 min and thereafter it proceeded at a slower rate and finally reached equilibrium. The dye uptake reached equilibrium within 15 min for 75 µmol/L and 75 min for 200 µmol/L RBV solutions, respectively. However, the data were taken for 120 min to ensure that complete equilibrium was established. As the initial concentration of the dye solution was increased from 75 to 200 µmol/L, the equilibrium dye adsorption (q_e) increased from 38.81 to 99.46 µmol/g (Table 1).

Table 1
Comparison of experimental and calculated q_e values, and kinetic parameters obtained from various kinetic models applied for the adsorption of RBV dye onto chitosan 10B at different solution pHs, initial concentrations of RBV, ionic strengths and temperatures

| Parameter	First-order kinetic model				Second-order kinetic model				Elovich model		
	$q_{e(exp)}$ (μmol/g)	k_1 (1/min)	$q_{e\,(cal)}$ (μmol/g)	R^2	k_2 (g/μmol min)	$q_{e(cal)}$ (μmol/g)	h (μmol/g min)	R^2	α (μmol/g min)	β (g/μmol)	R^2
pH											
4	58.25	0.1981	2.99	0.951	0.2113	58.14	714.29	1.000	1.46×10^{45}	1.8636	0.699
5	55.83	0.1193	4.72	0.901	0.0801	55.87	250.00	1.000	1.94×10^{23}	1.0324	0.887
6	54.17	0.1907	12.89	0.992	0.0498	54.35	147.16	1.000	4.57×10^{10}	0.5134	0.814
7	51.82	0.2515	28.11	0.989	0.0326	52.08	88.49	0.999	3.09×10^6	0.3429	0.791
8	50.51	0.1499	22.12	0.993	0.0179	51.02	46.73	0.999	2.34×10^4	0.2507	0.859
9	48.87	0.1122	27.79	0.999	0.0086	50.25	21.83	0.999	3.58×10^2	0.1660	0.911
10	44.89	0.1145	31.55	0.998	0.0070	46.73	15.31	0.999	0.96×10^2	0.1488	0.910
11	38.85	0.1199	32.70	0.998	0.0064	40.82	10.76	0.999	0.39×10^2	0.1479	0.901
12	31.78	0.1163	28.29	0.996	0.0067	33.67	7.55	0.999	0.22×10^2	0.1692	0.908
RBV (μmol/L)											
75	38.81	0.1453	5.74	0.879	0.0641	38.91	97.09	1.000	9.95×10^{10}	0.7472	0.689
100	52.32	0.1532	10.48	0.817	0.0380	52.63	105.26	1.000	2.69×10^7	0.3822	0.593
125	63.81	0.1336	13.13	0.872	0.0256	64.52	106.38	1.000	2.54×10^7	0.3094	0.673
150	75.18	0.1686	41.54	0.998	0.0103	76.34	60.24	0.999	8.18×10^3	0.1461	0.819
200	99.46	0.0797	54.11	0.998	0.0031	102.04	32.79	0.999	3.87×10^2	0.0767	0949
Ionic strength (mol/L)											
0.01	52.06	0.1096	5.52	0.955	0.0647	52.08	175.44	1.000	3.12×10^{15}	0.7587	0.763
0.02	51.81	0.1108	6.68	0.952	0.0527	52.08	142.86	1.000	4.62×10^{12}	0.6324	0.776
0.03	51.56	0.1177	7.69	0.944	0.0484	51.81	129.87	1.000	9.60×10^{10}	0.5576	0.759
0.04	51.31	0.1122	7.99	0.943	0.0438	51.54	116.28	1.000	1.69×10^{10}	0.5256	0.768
Temperature (°C)											
31	51.81	0.1343	9.76	0.909	0.0534	52.08	144.93	1.000	7.44×10^8	0.4550	0.526
36	52.06	0.1403	8.53	0.916	0.0640	52.36	175.44	1.000	3.83×10^{10}	0.5312	0.499
41	52.50	0.1294	7.16	0.873	0.0737	52.63	204.08	1.000	8.86×10^{11}	0.5892	0.529
46	52.88	0.0891	3.02	0.637	0.1323	52.91	370.37	1.000	1.06×10^{19}	0.9013	0.418
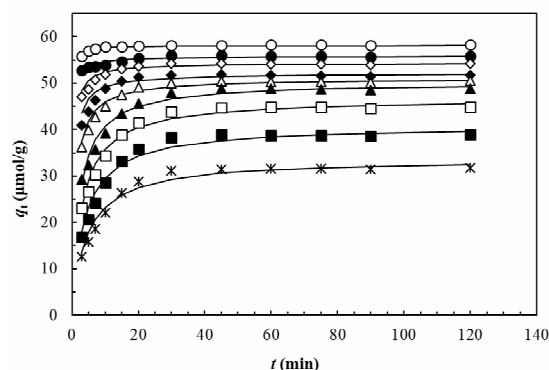
Figure 2: Adsorption kinetics of RBV onto chitosan 10B at various pH ([RBV]$_0$: 100 µmol/L; solution volume: 25 mL; chitosan 10B: 0.05 g; temperature: 31 °C; solution pHs: ○: pH 4; ●: pH 5; ◊: pH 6; ♦: pH 7; △: pH 8; ▲: pH 9; □: pH 10; ■: pH 11; *: pH12); (solid lines are generated numerically based on pseudo-second-order adsorption kinetic profiles using Eq. (4) and the values of q$_{e(cal)}$ and k$_2$ from Table 1)
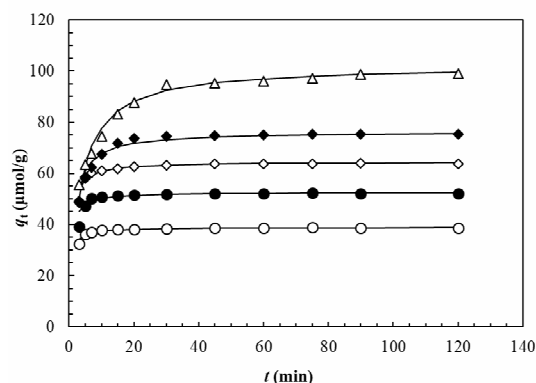
Figure 3: Adsorption kinetics of RBV onto chitosan 10B in aqueous solution (pH 4) at various initial dye concentrations (solution volume: 25 mL; chitosan 10B: 0.05 g; temperature: 31 °C; [RBV]$_0$: ○: 75 µmol/L; ●: 100 µmol/L; ◊: 125 µmol/L; ♦: 150 µmol/L; △: 200 µmol/L); (solid lines are generated numerically based on pseudo-second-order adsorption kinetic profiles using Eq. (4) and the values of q$_{e(cal)}$ and k$_2$ from Table 1)

The initial concentration of the dye solution affords a notable dynamic force to overwhelm the mass transfer resistance of all the molecules between the aqueous and solid phases.[20] Similar phenomena were also observed in the adsorption of Congo Red onto perlite[7] and Reactive Black 5 (RB5) onto chitosan[22] in aqueous solution, respectively.

Effect of ionic strength on adsorption kinetics

The presence of different salts in textile wastewater should be taken into consideration, since different salts (sodium sulphate, sodium chloride) are used in industrial dyeing in order to obtain uniform coloration. Therefore, various salts and metal ions could exist in wastewater and their concentration (ionic strength) affects significantly the performance of the adsorption process. In this study, sodium sulphate was used in varying salt concentration from 0.01 to 0.04 mol/L for dye solutions with an initial concentration of 100 µmol/L. Figure 4 shows important reductions in initial dye adsorption rate, h (µmol/g min), and the amount of equilibrium dye adsorption, q_e (µmol/g), with the increase in solution ionic strength (Table 1). The adsorption process is governed by electrostatic interactions between the cationic charged surface of chitosan 10B particles and anionic dye molecules. The decrease in the initial rate of dye adsorption and the amount of equilibrium dye adsorption could be due to an electrostatic screening effect, which is well known as electrostatic interaction between polycationic chitosan and SO_3^- anions. The structure of the diffuse layer is determined by electrostatic interactions described by the Gouy–Chapman theory and it is well known that the high ionic strength produces compression of the diffuse layer. These results are in agreement with those of other adsorption studies.[2,15,20]

Effect of temperature on adsorption kinetics

The effect of temperature on the adsorption kinetics of RBV onto chitosan 10B in aqueous solution (pH 4) is shown in Figure 5, where the initial concentration of the dye solution was 100 µmol/L. Below and above the equilibrium time, an increase in solution temperature leads to an increase in both the initial rate, h (µmol/g min), and the amount of equilibrium dye adsorption, q_e (µmol/g), (Table 1), which indicates a kinetically controlled endothermic adsorption process.[20] Therefore, higher temperatures facilitate the adsorption of RBV onto chitosan 10B flakes, because the mobility of dye molecules increased with rising solution temperature, and it suggests that the dye molecules interacted more effectively with the functional groups on chitosan flakes at high temperature.[19] Similar results were also observed in the adsorption of Reactive Yellow 145 and Reactive Black 5 onto chitosan in aqueous solutions, respectively.[20,22]

Kinetic analysis

The rate and the mechanism of the adsorption process can be elucidated on the basis of a kinetic study. The kinetics of RBV dye adsorption onto chitosan 10B in aqueous solution under various conditions may be explained by pseudo-first-order,[28] pseudo-second-order,[29] Elovich[30] and intraparticle diffusion[31] kinetic models, respectively. The pseudo-first-order rate expression is given as:

$$\log(q_e - q_t) = \log q_e - \frac{k_1}{2.303}t \tag{3}$$

where q_t (µmol/g) and q_e (µmol/g) are the amounts of dye adsorbed on chitosan 10B at time t and at equilibrium, respectively, and k_1 (1/min) is the rate constant of pseudo-first-order adsorption. A straight line of log $(q_e - q_t)$ *versus t* suggests the applicability of the pseudo-first-order kinetic model to fit the experimental data.
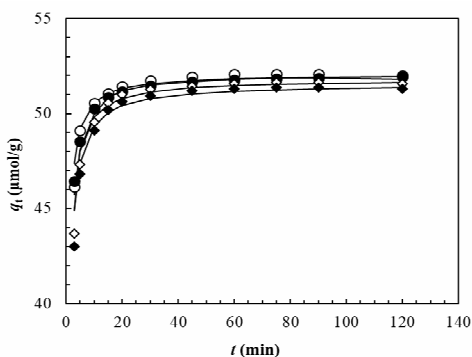
The pseudo-second-order kinetic model is

expressed as:

$$q_t = \frac{k_2 q_e^2 t}{(1 + k_2 q_e t)} \tag{4}$$

where k_2 (g/µmol min) is the rate constant of pseudo-second-order adsorption and can be determined from the linearized form of this equation, represented by Equation (5):

$$\frac{t}{q_t} = \frac{1}{k_2 q_e^2} + \frac{1}{q_e}t \tag{5}$$

If second-order kinetics is pertinent, the plot of t/q_t *versus* t should reveal a linear relationship. There is no need to know any parameter beforehand and the amount of equilibrium adsorption (q_e) can be calculated from Equation (5) and also, the initial adsorption rate, h (µmol/g min), can be obtained by:

$$h = k_2 q_e^2 \tag{6}$$

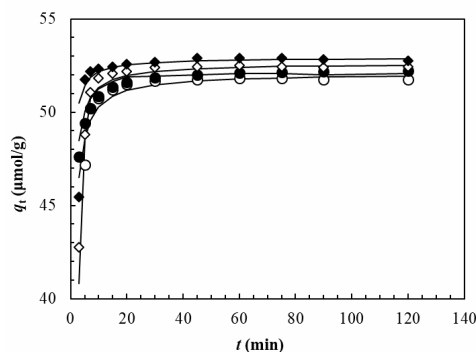Figure 4: Effects of ionic strength on adsorption kinetics of RBV onto chitosan 10B in aqueous solution ([RBV]$_0$: 100 µmol/L; solution volume: 25 mL; chitosan 10B: 0.05 g; temperature: 31 °C; ionic strength: ○: 0.01 mol/L; ●: 0.02 mol/L; ◊: 0.03 mol/L; ♦: 0.04 mol/L); (solid lines are generated numerically based on pseudo-second-order adsorption kinetic profiles using Eq. (4) and the values of q$_{e(cal)}$ and k$_2$ from Table 1)

Figure 5: Adsorption kinetics of RBV onto chitosan 10B in aqueous solution at various temperatures ([RBV]$_0$: 100 µmol/L; solution volume: 25 mL; chitosan 10B: 0.05 g; temperature: ○: 31 °C; ●: 36 °C; ◊: 41 °C; ♦: 46 °C); (solid lines are simulated pseudo-second-order adsorption kinetic profiles generated numerically using Eq. (4) and the values of q$_{e(cal)}$ and k$_2$ from Table 1)

The Elovich model has been also used to interpret the kinetics of adsorption. This model is useful in describing predominantly chemical adsorption onto highly heterogeneous adsorbents. The linear form of the Elovich equation is given by:

$$q_t = \frac{1}{\beta}\ln(\alpha\beta) - \frac{1}{\beta}\ln t \tag{7}$$

where α (µmol/g min) represents the initial adsorption rate and β (g/µmol) is related to the extent of surface coverage and the activation

energy for chemisorption. Elovich parameters α and β might be calculated from the plot of q_t *versus* ln t.

The values of correlation coefficients (R^2) and various kinetic parameters obtained from the applied kinetic models are shown in Table 1. The values of R^2 were ≤0.998 for the pseudo-first-order kinetics model and ≤0.949 for the Elovich model in all the cases. Also, the computed $q_{e(cal)}$ values achieved from the pseudo-first-order kinetic model do not give reasonable values,

which were too small compared with the experimental $q_{e(exp)}$ values (Table 1). These results suggest that the adsorption kinetics of RBV onto chitosan 10B in aqueous solution do not fit with the pseudo-first-order and Elovich models.

On the other hand, the slopes and y-intercepts of the plots of t/q_t *versus* t were used to calculate the pseudo-second-order rate constant (k_2) and q_e, respectively. The plots of t/q_t *versus* t showed straight lines, with good agreement with the experimental data taken for various solution pHs, initial dye concentrations, ionic strengths and temperatures. The values of R^2 for the pseudo-second-order kinetic model are ≥0.999 in almost

all the cases. The values of the calculated amount of equilibrium dye adsorption ($q_{e(cal)}$) also agree very well with the experimental values of $q_{e(exp)}$ (Table 1), indicating a favorable condition for pseudo-second-order adsorption kinetics.

The diffusion mechanism can be identified by using the intraparticle diffusion model proposed by Weber *et al*. in 1963.[31]

$$q_t = k_{id}\, t^{0.5} + I$$

(8)

where k_{id} (µmol/g min$^{0.5}$) is the intraparticle diffusion rate constant and I (µmol/g) is the intercept.
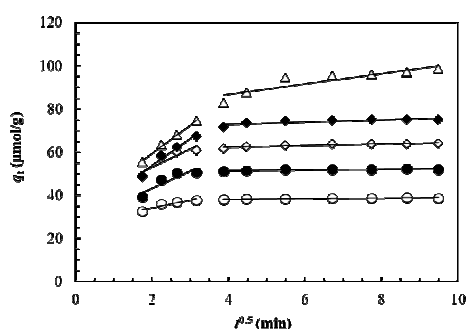

Figure 6: Intraparticle diffusion model plots for the adsorption of RBV dye on chitosan 10B at various initial concentrations (solution volume: 25 mL; chitosan 10B: 0.05 g; temperature: 31 °C; [RBV]$_0$: ○: 75 µmol/L; ●: 100 µmol/L; ◊: 125 µmol/L; ♦: 150 µmol/L; Δ: 200 µmol/L); (the constant values are listed in Table 2)
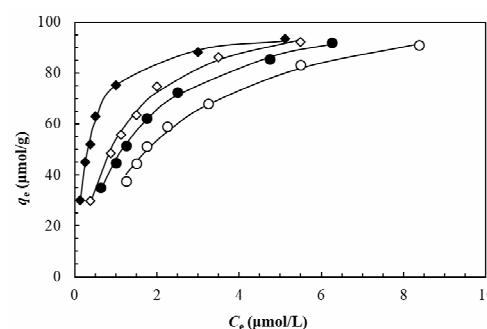

Figure 7: Typical equilibrium adsorption isotherm of RBV on chitosan 10B in aqueous solution at different temperatures ([RBV]$_0$: 75-200 µmol/L; solution volume: 25 mL; chitosan: 0.05 g; solution pH 4; temperatures: ○: 31 °C; ●: 36 °C; ◊: 41 °C; ♦: 46 °C); (solid lines are simulated Langmuir equilibrium adsorption isotherms at respective temperatures, generated using the Langmuir model in Eq. (19) and the Langmuir isotherm constants from Table 3)

Table 2
Diffusion rate parameters (k_{id1} and k_{id2}) for the adsorption of RBV onto chitosan 10B in aqueous solution under various conditions

Parameters	k_{id1} (µmol/g min$^{0.5}$)	I_1 (µmol/g)	R^2	k_{id2} (µmol/g min$^{0.5}$)	I_1 (µmol/g)	R^2
pH						
4	1.697	54.096	0.959	0.186	57.475	0.949
5	0.882	51.335	0.973	0.068	56.405	0.924
6	3.450	41.146	0.981	0.121	53.073	0.341
7	5.509	31.550	0.997	0.122	50.693	0.293
8	6.211	25.758	0.989	0.371	47.217	0.534
9	6.689	17.727	0.997	0.493	44.538	0.559
10	7.519	10.111	0.997	0.538	40.260	0.612
11	7.717	3.570	0.997	0.458	34.927	0.524
12	6.477	1.432	0.999	0.427	28.005	0.578
[RBV] (µmol/L)						
75	3.535	27.157	0.869	0.124	37.630	0.857
100	8.005	27.232	0.828	0.169	50.767	0.790
125	8.405	36.348	0.794	0.324	61.113	0.788
150	12.422	29.015	0.965	0.498	71.020	0.699
200	13.042	33.450	0.994	2.399	77.333	0.807

Ionic strength (mol/L)						
0.01	1.740	44.277	0.825	0.044	51.619	0.497
0.02	2.123	42.428	0.869	0.059	51.279	0.640
0.03	2.489	40.721	0.874	0.059	51.029	0.640
0.04	2.593	39.925	0.872	0.068	50.697	0.629
Temperatures (°C)						
31	5.073	33.841	0.696	0.032	51.479	0.464
36	4.462	36.408	0.671	0.025	51.809	0.674
41	3.967	38.469	0.717	0.026	52.149	0.362
46	2.660	43.564	0.531	0.028	52.565	0.274

The rate-controlling step is an intraparticle diffusion if the plot of the dye adsorbed (q_t) against the square root of contact time ($t^{0.5}$) leads to a straight line passing through the origin. When the plots do not pass through the origin, it is an indication of some degree of boundary layer control and the intraparticle diffusion is not the only rate-limiting step. In this case, the adsorption process is complex and more kinetic models that operate simultaneously may control the rate of dye adsorption.[20] The values of the intraparticle diffusion rate constant (k_{id}) were obtained from the linear part of the plots q_t *vs.* $t^{0.5}$ for RBV adsorption onto chitosan 10B in aqueous solution at various dye concentrations (Fig. 6).

In the range of initial dye concentration of 75-200 µmol/L, two separate regions are found in the plots (Fig. 6); namely, the first linear part can be attributed to the macropore diffusion (rate constant k_{id1}) and the second linear portion – to the micropore diffusion (rate constant k_{id2}). The values of k_{id1} and k_{id2} increase with increasing initial dye concentration (Table 2), which corresponds to an enhanced diffusion of the dye molecules from the outer surface of the adsorbent into macropores and micropores. Similar phenomena were also observed in the adsorption of Reactive Red 3 and Direct Brown 95 dyes onto chitosan.[21]

On the other hand, both k_{id1} and k_{id2} values decreased with the increase in solution temperatures (from 31 to 46 °C) (Table 2). In 2007, Cheung *et al.*[23] described analogous activities of chitosan towards acid dye and confirmed that during acid dye adsorption onto chitosan, the mechanism was predominantly intraparticle diffusion, but there was also a dependence on pore size, as the dye diffuses into macropores, mesopores and micropores, respectively.

The values of k_2 at different temperatures listed in Table 1 were used to estimate the activation energy for RBV adsorption onto chitosan 10B in aqueous solution. Assuming that the correlation among the rate constant (k_2), temperature (T) and activation energy (E_a) follows the Arrhenius equation, this would lead to the following expression:

$$ln k_2 = -\frac{E_a}{R}\left(\frac{1}{T}\right) + const. \tag{9}$$

where R is the gas constant (8.314 J/mol K). The slope of plot of $ln k_2$ *versus* $1/T$ ($R^2 = 0.996$) was used to evaluate E_a, which was estimated to be 25.52 kJ/mol for the adsorption of RBV onto chitosan 10B in aqueous solution in the temperature range of 31-46 °C, and initial dye concentration of 100 µmol/L. The chemisorption and physisorption mechanisms are frequently a principal sign to express the type of interaction between the dye molecule and the adsorbent. The physisorption processes typically have energies in the range of 4-40 kJ/mol, while higher activation energies (40-400 kJ/mol) suggest chemisorption.[20] Here, the obtained value of the activation energy (E_a: 25.52 kJ/mol) is low and thus, the sorption of RBV onto chitosan 10B in aqueous solution may be a physisorption process.

Equilibrium adsorption

Adsorption isotherms are preconditions to recognize the nature of the interaction between the adsorbate and the adsorbent used for the removal of organic pollutants. A plot of the amount of equilibrium dye adsorption, q_e (µmol/g), *versus* the liquid phase RBV equilibrium concentration, C_e (µmol/L), in aqueous solution (pH 4) at various temperatures is shown in Figure 7.

The amount of equilibrium dye adsorption onto chitosan 10B increased when the solution temperature was increased from 31 to 46 °C. The experimental data have been analyzed by Freundlich, Temkin, Dubinin-Radushkevich and Langmuir isotherm models, respectively.[32-35] The isotherm constants were obtained from the linearized plots of the respective isotherm

equations and the values of the correlation coefficients (R^2) are shown in Table 3.

Freundlich isotherm

The well-known Freundlich isotherm is based on sorption to a heterogeneous surface or surfaces supporting sites of varied affinities. It is assumed that the stronger binding sites are occupied first and that the binding strength decreases with an increasing degree of site occupation. The Freundlich equation is given as:

$$q_e = K_F C_e^{\frac{1}{n}}$$

(10)

Equation (10) can be linearized by taking the logarithms to find out the parameters K_F and $1/n$.

$$\ln q_e = \frac{1}{n} \ln C_e + \ln K_F$$

(11)

where K_F is roughly an indicator of the adsorption capacity ($(\mu mol/g)(\mu mol/L)^{-1/n}$) and n is related to the intensity of adsorption. K_F and n can be determined from the linear plot of $\ln q_e$ *versus* $\ln C_e$. The calculated results are listed in Table 3. The magnitude of the exponent n gives an indication of the favorability of adsorption. From Table 3, the exponent n is larger than 1 for the adsorption of RBV by chitosan 10B in aqueous solution at different temperatures, indicating favorable adsorption conditions.[36]

Temkin isotherm

Temkin isotherm contains a factor that explicitly takes into account the adsorbing species–adsorbate interactions. This isotherm assumes that: (i) the heat of adsorption of all the molecules in the layer decreases linearly with coverage due to adsorbent–adsorbate interactions, and (ii) adsorption is characterized by a uniform distribution of binding energies. The Temkin isotherm is represented by the following equation:

$$q_e = \left(\frac{RT}{b}\right) \ln(K_T C_e)$$

(12)

Equation (12) can be expressed in its linear form as:

$$q_e = B_1 \ln K_T + B_1 \ln C_e$$

(13)

where:

$$B_1 = \frac{RT}{b}$$

(14)

and K_T ($\mu mol/L$) is the Temkin isotherm constant, b (J/mol) is a constant related to the heat of sorption, R is the gas constant (8.314 J/mol K) and T is the absolute temperature (K). A plot of q_e *versus* $\ln C_e$ enables the determination of the isotherm constants b and K_T from the slope and intercept, respectively. The calculated parameters and correlation coefficients are listed in Table 3. The heat of adsorption changed linearly with coverage due to adsorbent–adsorbate interaction. The correlation coefficients (R^2) of the Temkin isotherm are 0.989, 0.994, 0.988, and 0.972 at 31, 36, 41 and 46 °C, respectively. The poor correlation coefficient values showed that the experimental data were not in good agreement with the Temkin model.

Dubinin-Radushkevich isotherm

The Dubinin-Radushkevich isotherm equation used to estimate the characteristic porosity of the adsorbent and the apparent energy of adsorption, which is given by Equation (15):

$$q_e = q_{DR} \exp(-K_{DR} \varepsilon^2)$$

(15)

Equation (15) can be expressed in its linear form as:

$$\ln q_e = \ln q_{DR} - K_{DR} \varepsilon^2$$

(16)

Polanyi potential (ε) is given as Equation (17):

$$\varepsilon = RT \ln\left(1 + \frac{1}{C_e}\right)$$

(17)

The plot of $\ln q_e$ *versus* ε^2 gives a straight line with a slope of $-K_{DR}$ and an intercept of $\ln q_{DR}$. The Dubinin-Radushkevich constant can give valuable information regarding the mean energy of adsorption by Equation (18):

$$E = \frac{1}{(2K_{DR})^{0.5}}$$

(18)

The calculated parameters and correlation coefficients are listed in Table 3. The correlation coefficients (R^2) of the Dubinin-Radushkevich isotherm are 0.978, 0.918, 0.915 and 0.968 at 31, 36, 41 and 46 °C, respectively. The poor correlation coefficient values showed that the experimental data were not in good agreement with the Dubinin-Radushkevich model.

Meanwhile, from the Dubinnin-Radushkevich isotherm, the mean adsorption energy (E) involved the transfer of the free energy of one mole of solute from infinity (in solution) to the adsorbent surface. The adsorption behavior might have predicted the physical adsorption in the range of 1-8 kJ/mol of the mean adsorption energy, and the chemical adsorption in more than 8 kJ/mol of the mean adsorption energy.[37,38] The mean adsorption energies (E) for the adsorption of RBV onto chitosan 10B in aqueous was found to

be in the range from 1.118 to 4.082 kJ/mol, which indicates that the present dye adsorption predominates over the physical adsorption process.

Langmuir isotherm

The commonly used Langmuir isotherm has found successful application in many real sorption processes and is expressed as:

$$q_e = \frac{K_L C_e}{(1 + a_L C_e)} \tag{19}$$

The constants K_L and a_L are the characteristics of the Langmuir equation and can be determined from the linearized form of this equation, represented by Equation (20):

$$\frac{C_e}{q_e} = \frac{1}{K_L} + \frac{a_L}{K_L} C_e \tag{20}$$

Therefore, the plot of C_e/q_e *versus* C_e gives a straight line with the slope a_L/K_L and y-intercept $1/K_L$. The constant a_L is the Langmuir equilibrium constant and the ratio a_L/K_L gives the inverse of theoretical monolayer saturation capacity (q_m). The values of a_L and K_L were computed from the slopes and y-intercepts of different linearized plots of (C_e/q_e) *versus* C_e represented at different temperatures. The calculated results are shown in Table 3.

The fits are quite good for all the four different temperatures under the concentration range studied (correlation coefficient, $R^2 \geq 0.989$). Comparing the linear correlation coefficients listed in Tables 3, it could also be concluded that the equilibrium adsorption of RBV dye onto chitosan 10B in aqueous solution fitted very well with the Langmuir isotherm equation. The high degree of the linear correlation coefficient (R^2) also suggests that a single surface reaction with constant activation energy is the predominant sorption step and possibly the predominant rate-controlling step.[39]

Table 3
Freundlich, Temkin, Dubinin-Radushkevich and Langmuir isotherm constants at different temperatures and thermodynamic parameters for the adsorption of dye RBV onto chitosan in aqueous solution at pH 4

Parameters	Freundlich isotherm			
T (°C)	31	36	41	46
K_F ((µmol/g) (µmol/L)$^{-1/n}$)	37.993	45.801	50.360	66.062
N	2.241	2.409	2.347	3.497
R^2	0.951	0.969	0.953	0.906
Parameters	Temkin isotherm			
T (°C)	31	36	41	46
K_T (µmol/L)	3.417	3.874	4.056	7.420
b (J/mol)	90.811	101.715	106.882	155.416
R^2	0.989	0.994	0.986	0.972
Parameters	Dubinin-Radushkevich isotherm			
T (°C)	31	36	41	46
q_{DR} (µmol/g)	87.400	83.029	82.426	85.841
K (J^2/mol^2)	4.000×10^{-7}	2.000×10^{-7}	9.000×10^{-8}	3.000×10^{-8}
E (kJ/mol)	1.1180	1.5811	2.3570	4.0824
R^2	0.978	0.918	0.915	0.968
Parameters	Langmuir isotherm			
T (°C)	31	36	41	46
K_L (L/g)	49.019	78.125	104.167	322.581
a_L (L/µmol)	0.4167	0.6953	0.9375	3.2903
q_m (µmol/g)	117.65	112.36	111.11	98.04
R_L	0.012	0.007	0.005	0.002
R^2	0.989	0.998	0.989	0.999
Thermodynamic parameters				
T (°C)	31	36	41	46
ΔG (kJ/mol)	−32.71	−34.56	−35.89	−39.79
ΔH (kJ/mol)		104.39		
ΔS (J/K mol)		449.85		
R^2		0.904		

Table 4
Relation between value of R_L and type of adsorption

Value of R_L	Type of adsorption
$R_L > 1.0$	Unfavorable
$R_L = 1.0$	Linear
$0 < R_L < 1.0$	Favorable
$R_L = 0$	Irreversible

From the results shown in Table 3, the capacities of chitosan for dye adsorption are dependent on the solution temperatures. The values of a_L and K_L increased when the solution temperature was increased from 31 to 46 °C. These results also suggest that the chitosan–RBV interaction must be an endothermic process.

The basic features of the Langmuir isotherm can be stated in terms of the dimensionless constant separation factor (R_L),[40] which is defined as Equation (21):

$$R_L = \frac{1}{(1 + a_L C_0)}$$
(21)

where a_L is the Langmuir equilibrium constant and C_0 is the highest initial dye concentration (µmol/L). According to the value of R_L, the isotherm shape may be interpreted as described in Table 4. The values of R_L were calculated to be in the range between 0 and 1 at 31, 36, 41 and 46 °C, respectively, which indicates that the adsorption is favorable at all the temperatures.

Moreover, in an effort to understand the equilibrium processes involved in RBV adsorption onto chitosan 10B, a computer simulation of the adsorption isotherms has been performed numerically on the basis of the Langmuir model in Equation (19) and using the Langmuir isotherm constants listed in Table 3, and the results were compared with the experimental data (Fig. 7). The observed curves were obtained from the plots of equilibrium adsorption, q_e (µmol/g), *versus* the liquid phase RBV equilibrium concentration, C_e (µmol/L), at different temperatures. The simulated curves (all the solid lines) were obtained as described. The observed data are well reproduced in the simulated data, as shown in Figure 7, supporting that all the isotherm data are described well by the Langmuir equation. A comparison of maximum RBV dye adsorption onto various adsorbents reported in the literature[41-44] is shown in Table 5. Chitosan 10B is found to be an efficient and promising adsorbent to remove RBV from aqueous solution.

Reuse of chitosan

The typical phenomena of RBV dye adsorption-desorption-adsorption onto chitosan 10B flakes in aqueous solution are shown in Figure 8. In the adsorption step, the initial dye concentration was 100 µmol/L, with a solution pH 4.0 and a temperature of 31 °C, whereas the release of RBV from the dye-loaded chitosan 10B was carried out in 0.1 M NaOH solution at pH 12.5 and temperature of 31 °C. It was observed that the amount of equilibrium dye adsorption was 58.25 µmol/g in the first adsorption step, which was maintained for 120 min. The dye desorption rate was rapid for the first 30 min and 73% of RBV dye was released from the dye-loaded chitosan within 40 min. After 120 min of desorption, 90% of the dye was liberated from the RBV-loaded chitosan. This may be due to the fact that in a basic solution, the positively charged amino groups of chitosan 8B are deprotonated, and the electrostatic interaction between chitosan and dye molecules becomes much weaker.[22] Following the desorption step, the second adsorption step took place and it repeated the similar dynamical shape of the first adsorption step. It takes 120 min to adsorb a similar amount of RBV dye to that of desorption, and the total amount of dye adsorption is similar to that of the first adsorption step. These results show that our chitosan flakes can be reused for further dye adsorption.

Thermodynamics

The thermodynamic parameters, such as changes in free energy (ΔG), enthalpy (ΔH) and entropy (ΔS), were determined using the following equations:[23]

$$\Delta G = -RT \ln a_L$$
(22)

$$\ln a_L = \frac{\Delta S}{R} - \frac{\Delta H}{RT}$$
(23)

where a_L (L/mol) is the equilibrium constant in Table 3, T is the solution temperature (K), and R is the gas constant (8.314 J/mol K). ΔH and ΔS were calculated from the slope and y-intercept of

van't Hoff plot of $\ln a_L$ *versus* $1/T$ (correlation coefficient $R^2 = 0.904$). The results are presented in Table 3. The change in enthalpy (ΔH) for the adsorption of RBV onto chitosan 10B in aqueous solution was estimated to be 104.39 kJ/mol. The positive value of ΔH suggests that the adsorption of RBV by chitosan 10B is endothermic, which is supported by the increasing adsorption of RBV with the increase in temperature, while a negative value of ΔG and a positive value of ΔS indicate that the adsorption reaction is a spontaneous process and more favorable at high temperature.[22] Generally, the absolute magnitude of the change in free energy for physical adsorption is smaller than that of chemisorption.

Table 5
A comparison of maximum RBV dye adsorption onto various adsorbents

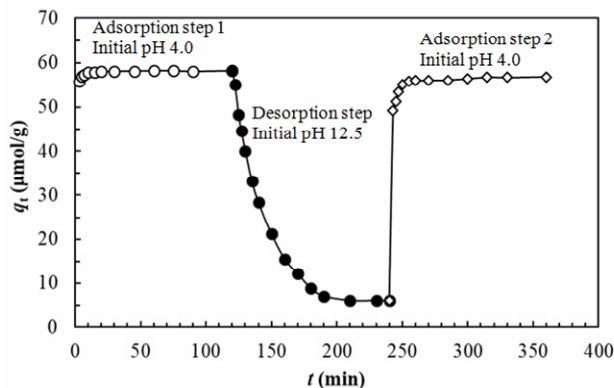| Adsorbent	Temperature (°C)	pH	q_m (μmol/g)	References
Chitosan 10B	31	4	117.65	This work
Granular activated carbon (GAC)	70	2.5	18.49	41
Chitin	70	2.5	51.93	41
Radish leaves (RL)	70	2.5	54.38	41
Crosslinked poly(N-vinylpyrolidone) (CPVP)	25		0.14	42
Natural rice hull (RHI)	10	2	96.74	43
Treated rice hull (RHT)	55	2	92.27	43
Cocoa pod husk	-	-	49.21	44

Figure 8: Adsorption and desorption kinetics of RBV on chitosan 10B in aqueous solution at 31 °C and 100 μmol/L initial dye concentration in three steps: adsorption step 1 at initial pH 4.0, desorption step at initial pH 12.5, and adsorption step 2 at initial pH 4.0

The former ranges from -20 to 0 kJ/mol, and the latter ranges from -80 to -400 kJ/mol.[22] When the temperature was increased from 31 to 46 °C, ΔG increased from -32.71 to -39.79 kJ/mol. This could be considered as physical adsorption and more favorable at high temperature, which is supported by the small value of E_a (25.52 kJ/mol) for the adsorption of RBV onto chitosan 10B. In addition, the considerably low ΔG values illustrate saturation in the adsorption process.[45] In 2010, Nawi *et al*. also reported a similar observation for the adsorption of Reactive Red 4 by immobilized chitosan on glass plates.[46]

CONCLUSION

The adsorption of RBV onto chitosan 10B flakes in aqueous solution was systematically investigated under various conditions. Batch adsorption experiments proved that the solution pH, initial concentration of the dye solutions, ionic strengths and solution temperature significantly influence the initial sorption rate and the amount of equilibrium RBV dye adsorption onto chitosan 10B flakes. The adsorption kinetics could be explained adequately by the pseudo-second-order model, while intraparticle diffusion played an important role in the rate-limiting step.

The experimental sorption kinetic profiles were perfectly reproduced in the simulated data obtained from numerical analysis on the basis of the pseudo-second-order kinetic model in Equation (4), using the values of k_2 and $q_{e(cal)}$ listed in Table 2. Equilibrium adsorption isotherms correlated reasonably well with the Langmuir model, compared to the Freundlich, Temkin and Dubinin-Radushkevich models. Thermodynamic analyses indicated that the adsorption of RBV onto chitosan 10B flakes was endothermic and spontaneous, additionally, the adsorption of RBV onto chitosan 10B flakes was produced *via* a physisorption process.

A significant amount (90%) of RBV dye was released from the dye-loaded chitosan in 0.1 M NaOH solution (pH 12.5) and the chitosan flakes could be reused. This study concludes that the readily available chitosan 10B could be used as an appropriate adsorbent for removing reactive dyes from wastewater.

REFERENCES
[1] E. Eren, *Clean*: *Soil Air Water*, **38**, 758 (2010), https://doi.org/10.1002/clen.201000060
[2] S. Chatterjee, S. Chatterjee, B. P. Chatterjee and A. K. Guha, *Colloid. Surf. A.*, **299**, 146 (2007), https://doi.org/10.1016/j.colsurfa.2006.11.036
[3] M. S. Chiou and H. Y. Li, *Chemosphere*, **50**, 1095 (2003), https://doi.org/10.1016/S0045-6535(02)00636-7
[4] B. Armagan, M. Turan and M. Celik, *Desalination*, **170**, 33 (2004), https://doi.org/10.1016/j.desal.2004.02.091
[5] T. S. Anirudhan and M. Ramachandran, *J. Colloid Interface Sci.*, **299**, 116 (2006), https://doi.org/10.1016/j.jcis.2006.01.056
[6] T. Ngulube, J. R. Gumbo, V. Masindi and A. Maity, *J. Environ. Manag.*, **191**, 35 (2017), https://doi.org/10.1016/j.jenvman.2016.12.031
[7] G. Vijayakumar, M. Dharmendrirakumar, S. Renganathan, S. Sivanesan, G. Baskar *et al.*, *Clean*: *Soil Air Water*, **37**, 355 (2009), http://doi.org.

[8] A. Khaled, A. El-Nemr, A. El-Sikaily and O. Abdelwahab, *Desalination*, **238**, 210 (2009), https://doi.org/10.1016/j.desal.2008.02.014
[9] W. M. A. El-Rahim, O. A. M. El-Ardy and F. H. A. Mohammad, *Desalination*, **249**, 1206 (2009), https://doi.org/10.1016/j.desal.2009.06.037
[10] N. Kannan and M. M. Sundaram, *Dyes Pigments*, **51**, 25 (2001), https://doi.org/10.1016/S0143-7208(01)00056-0
[11] F. Rozada, L. F. Calvo, A. I. García, J. Martín-Villacorta and M. Otero, *Bioresour. Technol.*, **87**, 221 (2003), https://doi.org/10.1016/S0960-8524(02)00243-2
[12] B. H. Hameed, A. A. Ahmad and N. Aziz, *Desalination*, **247**, 551 (2009), https://doi.org/10.1016/j.desal.2008.08.005
[13] E. Caglar, Y. O. Donari, A. Sinag, I. Birogul, S. Bilge *et al.*, *Turk. J. Chem.*, **42**, 86 (2018).
[14] T. Murugan, A. Ganapathi and R. Valliappan, *E. J. Chem.*, **7**, 669 (2010).
[15] A. K. Kushwaha, N. Gupta and M. C. Chattopadhyaya, *J. Saudi Chem. Soc.*, **18**, 200 (2014), doi: 10.1016/j.jscs.2011.06.011
[16] A. A. Inyinbor, F. A. Adekola and G. A. Olatunji, *S. Afr. J. Chem.*, **68**, 115 (2015), http://dx.doi.org/10.17159/0379-4350/2015/v68a17
[17] S. Banerjee and M. C. Chattopadhyaya, *Arabian J. Chem.*, **10**, S1629 (2017), https://doi.org/10.1016/j.arabjc.2013.06.005
[18] L. Liu, R. Wang, J. Yu, L. Hu, Z. Wang *et al.*, *RSC Adv.*, **8**, 15804 (2018), DOI: 10.1039/C8RA01563E
[19] R. Huang, Q. Liu, J. Huo and B. Yang, *Arabian J. Chem.*, **10**, 24 (2017), https://doi.org/10.1016/j.arabjc.2013.05.017
[20] S. Karmaker, T. Sen and T. K. Saha, *Polym. Bull.*, **70**, 2047 (2015).
[21] M. Ignat, V. Dulman and T. Onofrei, *Cellulose Chem. Technol.*, **46**, 357 (2012), http://www.cellulosechemtechnol.ro/pdf/CCT5-6(2012)/p.357-367.pdf
[22] T. K. Saha, N. C. Bhoumik, S. Karmaker, M. G. Ahmed, H. Ichikawa *et al.*, *Clean*: *Soil Air Water*, **39**, 984 (2011), DOI: 10.1002/clen.201000315
[23] W. H. Cheung, Y. S. Szeto and G. McKay, *Bioresour. Technol.*, **98**, 2897 (2007), https://doi.org/10.1016/j.biortech.2006.09.045
[24] H. Ansari, M. Miralinaghi and F. Azizinezhad, *Cellulose Chem. Technol.*, **52**, 191 (2019), http://www.cellulosechemtechnol.ro/pdf/CCT1-2(2019)/p.191-204.pdf
[25] K. Gul, S. Sohni, M. Waqar, F. Ahmad, N. A. N. Norulaini *et al.*, *Carbohyd. Polym.*, **152**, 520 (2016), https://doi.org/10.1016/j.carbpol.2016.06.045
[26] J. O. Goncalves, J. P. Santos, E. C. Rios, M. M. Crispim, G. L. Dotto *et al.*, *J. Mol. Liq.*, **225**, 265 (2017), https://doi.org/10.1016/j.molliq.2016.11.067
[27] M. Khan and A. K. M. A. Nowsad, *J. Bangladesh Agric. Univ.*, **10**, 367 (2012),

https://doi.org/10.3329/jbau.v10i2.14930

28   S. Lagergren, *K. Sven. Vetenskapsakad. Handl.*, **24**, 1 (1898).

29   G. McKay and Y. S. Ho, *Process Biochem.*, **34**, 451 (1999), https://doi.org/10.1016/S0032-9592(98)00112-5

30   S. Y. Elovich and O. G. Larinov, *Izv. Akad. Nauk SSSR, Otd. Khim. Nauk*, **2**, 209 (1962).

31   W. J. Weber, J. C. Morris and J. Sanit, *J. Sanit. Eng. Div.*, *Proc. Am. Soc. Civ. Eng.*, **89**, 31 (1963).

32   H. Freundlich, *Z. Phys. Chem.*, **57**, 384 (1906).

33   M. I. Temkin and V. Pyzhev, *Acta Physiochim.*, **12**, 327 (1940).

34   A. A. Inyinbor, F. A. Adekola and G. A. Olatunji, *Water Resour. Ind.*, **15**, 14 (2016), https://doi.org/10.1016/j.wri.2016.06.001

35   I. Langmuir, *J. Am. Chem. Soc.*, **40**, 1361 (1918), https://doi.org/10.1021/ja02242a004
G. McKay, H. S. Blair and J. R. Gardner, *J. Appl. Polym. Sci.*, **27**, 3043 (1982), https://doi.org/10.1002/app.1982.070270827

36   A. H. Chen, S. C. Liu, C. Y. Chen and C. Y. Chen, *J. Hazard. Mater.*, **154**, 184 (2008), https://doi.org/10.1016/j.jhazmat.2007.10.009

37   A. H. Chen, C. Y. Yang, C. Y. Chen, C. Y. Chen and C. W. Chen, *J. Hazard. Mater.*, **163**, 1068 (2009), https://doi.org/10.1016/j.jhazmat.2008.07.073

38   Y. C. Wong, Y. S. Szeto, W. H. Cheung and G. McKay, *Langmuir*, **19**, 7888 (2003), https://doi.org/10.1021/la030064y

39   K. R. Hall, L. C. Eagleton, A. Acrivers and T. Vermenlem, *Ind. Eng. Chem. Fundam.*, **5**, 212 (1966).

40   R. Sanghi and B. Bhattacharya, *J. Sci. Ind. Res.*, **61**, 432 (2002), http://hdl.handle.net/123456789/26358

41   S. Ekici, Y. Isikver, N. Sahiner and D. Saraydin, *Adsorpt. Sci. Technol.*, **21**, 651 (2003), https://doi.org/10.1260/026361703772776439

42   G. A. C. Ribeiro, D. S. A. Silva, C. C. dos Santos, A. P. Vieira, C. W. B. Bezerra *et al.*, *Polimeros*, **27**, 16 (2017).

43   O. S. Bello, T. T. Siang and M. A. Ahmad, *Asia-Pac. J. Chem. Eng.*, **7**, 378 (2012), https://doi.org/10.1002/apj.557

44   S. Chatterjee, S. Chatterjee, B. P. Chatterjee, A. R. Das and A. K. Guha, *J. Colloid Interfac. Sci.*, **288**, 30 (2005), https://doi.org/10.1016/j.jcis.2005.02.055

45   M. A. Nawi, S. Sabar, A. H. Jawad, Sheilatina and W. S. W. Ngah, *Biochem. Eng. J.*, **49**, 317 (2010), https://doi.org/10.1016/j.bej.2010.01.006